LBL-31049
Preprint

# Lawrence Berkeley Laboratory

UNIVERSITY OF CALIFORNIA

## Accelerator & Fusion Research Division

Submitted to Physics of Fluids B

**Electromagnetic Instability of the Ion-Focused Regime**

D.H. Whittum

July 1991

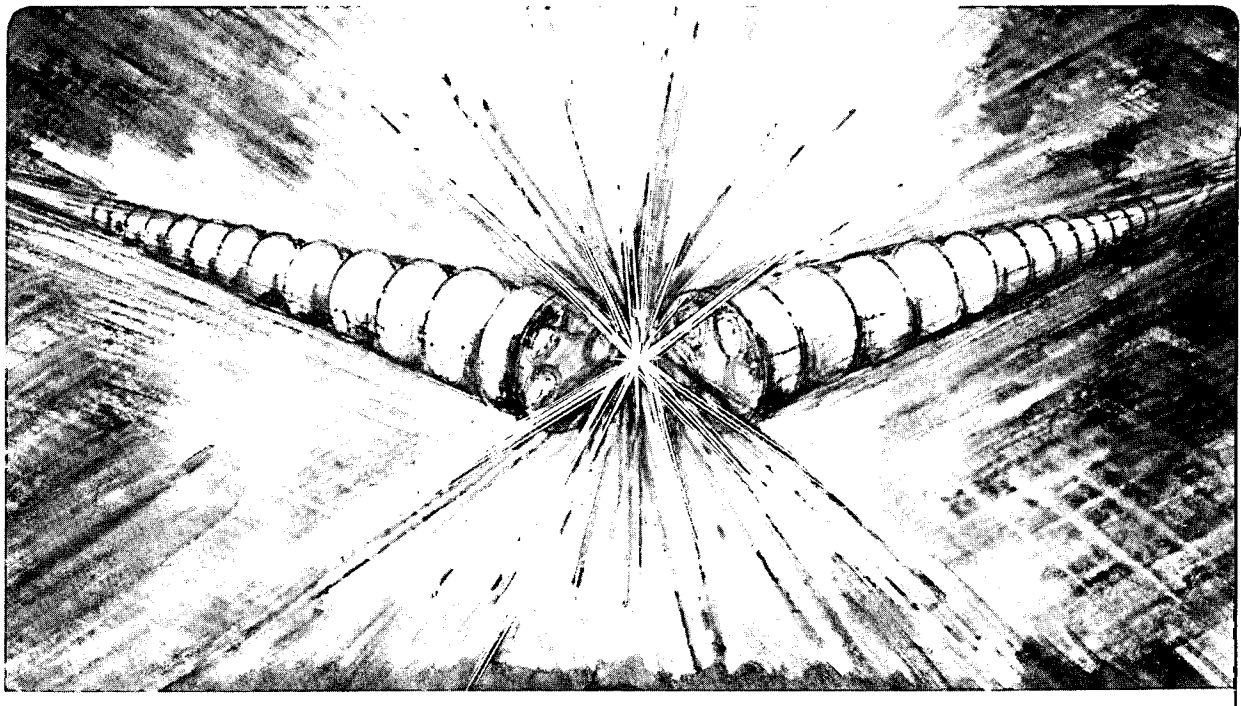

LOAN COPY
Circulates
for 4 weeks
LBL-31049
Copy 2
Bldg. 50 Library.

Prepared for the U.S. Department of Energy under Contract Number DE-AC03-76SF00098

## DISCLAIMER

This document was prepared as an account of work sponsored by the United States Government. While this document is believed to contain correct information, neither the United States Government nor any agency thereof, nor the Regents of the University of California, nor any of their employees, makes any warranty, express or implied, or assumes any legal responsibility for the accuracy, completeness, or usefulness of any information, apparatus, product, or process disclosed, or represents that its use would not infringe privately owned rights. Reference herein to any specific commercial product, process, or service by its trade name, trademark, manufacturer, or otherwise, does not necessarily constitute or imply its endorsement, recommendation, or favoring by the United States Government or any agency thereof, or the Regents of the University of California. The views and opinions of authors expressed herein do not necessarily state or reflect those of the United States Government or any agency thereof or the Regents of the University of California.

LBL-31049

# Electromagnetic instability of the ion-focused regime

**David H. Whittum***

*Lawrence Berkeley Laboratory, University of California, Berkeley, California 94720*

July 1991

* Work at LBL was supported by the Director, Office of Energy Research, Office of High Energy and Nuclear Physics, Division of High Energy Physics, of the US Department of Energy under contract DE-AC03-76SF00098. Work in Japan was supported by the XIV International Conference on high Energy Accelerators, the National Laboratory for High Energy Physics (KEK), and a postdoctoral award from the Japan Society for the Promotion of Science, in cooperation with the National Science Foundation.

# Electromagnetic instability of the ion-focused regime

David H. Whittum[a]
Lawrence Berkeley Laboratory,
University of California, Berkeley, California 94720

(Received )

A relativistic electron beam propagating through a wide plasma channel in the ion-focused regime exhibits an electromagnetic instability coupled to the "betatron" motion, with peak growth rate near a resonant angular frequency $\omega \sim 2\gamma^2\omega_\beta$, where $\gamma$ is the Lorentz factor for the beam, and $\omega_\beta$ is the angular frequency of transverse oscillations. An eikonal formalism is derived and applied to compute the dispersion relation and to follow instability growth through saturation. The effect of detuning spread on gain is examined. Analytic scaling laws are compared to the results of numerical simulation for a practical example corresponding to a high-gain microwave amplifier. Constraints due to competing instabilities and scattering are noted and the extension to short wavelengths is discussed.

PACS: 42.55.Tb, 52.40Mj, 41.80Ee.

## I. INTRODUCTION

The "ion-focused" regime[1] (IFR) of transport for relativistic electrons beams in plasmas has been described in detail by Buchanan,[2] as the limit in which an intense beam, propagating through a radially finite plasma channel, less dense than the beam core ("underdense"), expels all free plasma electrons to large radii. For typical applications of the IFR,[3,4] the plasma channel is intentionally made *narrow*, with a width of order the equilibrium beam radius so that focussing of beam electrons is nonlinear and instabilities which routinely arise in transport may be damped. In this work the opposite limit is considered, where the plasma channel is *wide*, and focussing is approximately *linear*. It will be shown that under certain conditions, an electromagnetic instability results, so that a wave propagating with the beam and resonant with the transverse betatron motion may be amplified.

This instability has been proposed as the basis for a novel "free-electron" laser,[5,6,7] and in this work issues alluded to previously will be considered in detail. In Sec. II, an eikonal formalism is derived describing instability growth through saturation. The dispersion relation is calculated. In Sec. III, the cold-beam dispersion relation is studied, and finite temperature ("detuning spread") effects are assessed. In Sec. IV the scaling laws of Sec. III are compared to the results of numerical simulation for a practical numerical example, corresponding to a high-gain microwave amplifier. Deleterious plasma effects are noted. In Sec. V conclusions are offered and some problems for future work are discussed.

## II. EIKONAL FORMALISM

### A. Approximations

In a typical ion-focusing experiment, the beamline is backfilled with a working gas such as benzene or diethlyaniline and a plasma channel is created along the center of the beamline by an excimer laser pulse.[8] We consider propagation of a relativistic electron beam through such a channel in the limit $n_p < n_b$, where $n_b$ is beam density, $n_p$ is the plasma electron density. It is assumed that the laser-produced charge per unit length is less than that of the beam, so that all free plasma electrons are expelled to the beam-pipe, by the beam head as it propagates down the beamline, in the axial $(+z)$ direction, as depicted in Fig. 1. The very massive ions are left fixed and focus the remainder of the beam. It is assumed that the beam pulse length $T$ is short compared to the time for ions to neutralize the beam, *i.e.*, $\omega_i T << 1$ where $\omega_i$ is the ion-plasma frequency, $\omega_i^2 = 4\pi n_p e^2/m_i$, with $m_i$ the ion mass and $e$ the ion charge. In addition, the more rapid "slosh" motion of ions near the beam will be neglected. This motion occurs on a time scale $2\pi/\omega_s$, where $\omega_s^2 = 4\pi n_b e^2/m_i$. It is also assumed that self-fields perturb beam electron motion negligibly and this imposes the Budker condition[1] on the plasma density, $n_p >> n_b/\gamma^2$, where $\gamma$ is the Lorentz factor for the beam.

With these approximations, the transverse motion of a beam electron is governed by the Hamiltonian,

$$H_\perp \approx \frac{p_x^2}{2p_z} + \frac{p_y^2}{2p_z} + \frac{1}{4}k_p^2(x^2 + y^2) \tag{1}$$

corresponding to a relativistic, 2-D, simple harmonic oscillator. Here $x$ and $y$ are the transverse coordinates, with $p_x$, and $p_y$ the corresponding momenta. We adopt the convention that momenta are normalized by $mc$ and energies by $mc^2$, where $c$ is the speed of light, and $m$ is the electron mass. The axial momentum is $p_z$ and is a constant of the motion. The quantity $k_p = \omega_p / c$, with $\omega_p$ the plasma frequency, $\omega_p^2 = 4\pi n_p e^2/m$. Beam electrons oscillate transversely at the "betatron frequency" $\omega_\beta \sim \omega_p/(2p_z)^{1/2}$.

## B. Perturbed Particle Equations

Next consider the effect of an externally supplied electromagnetic wave, linearly polarized in the $y$-direction, propagating with the beam as depicted in Fig. 2. The vector potential may be expressed in terms of dimensionless amplitude and phase, $A$ and $\varphi$, as

$$A_y = \frac{mc^2}{e} A \sin(\zeta) , \tag{2}$$

$$\zeta = k_z z - \omega t + \varphi . \tag{3}$$

The angular frequency is $\omega$ and the axial wavenumber is $k_z$. The eikonal $A exp(i\varphi)$ is assumed to vary slowly in $t$ on the $\omega^{-1}$ scale, and in $z$ on the $k_z^{-1}$ scale, and to vary negligibly transversely within the beam.

The single-particle Hamiltonian is,

$$H \approx p_z + \frac{1}{2\,p_z} + \frac{p_x^2}{2\,p_z} + \frac{p_y^2}{2\,p_z} + \frac{1}{4}k_p^2(x^2+y^2) + \frac{p_y}{p_z}A\,sin(\zeta) \quad , \tag{4}$$

where $A<<1$ is assumed. The quantities $p_x$, $p_y$, and $p_z$ are the canonical momenta in $x$, $y$, and $z$, respectively,

$$p_x = \gamma\beta_x \ , \tag{5}$$

$$p_y = \gamma\beta_y - \frac{e}{mc^2}A_y \ , \tag{6}$$

$$p_z = \gamma\beta_z - \frac{e}{mc^2}A_z \ , \tag{7}$$

$$\gamma = \left\{1 - \beta_x^2 - \beta_y^2 - \beta_z^2\right\}^{-1/2} \ . \tag{8}$$

and $p_z>>p_x$, $p_y$, is assumed. The particle velocity components normalized by $c$ are $\beta_x$, $\beta_y$, and $\beta_z$. The axial vector potential $A_z$ arises from the axial beam current, and results in a fractional correction to $p_z$ of order $v/p_z<<1$, where $v=I/I_0$ is Budker's parameter,[1] with $I_0=mc^3/e\sim17$kA, and $I$ the beam current. This small term will be neglected for now and discussed further in Sec. III in connection with "detuning spread".

The equations of motion derived from the Hamiltonian of Eq. (4) describe an electron drifting in $z$, subject to an axial "$VxB$" force as it oscillates in the potential well

$$\frac{dz}{d\tau} = 1 - \frac{1}{2\,p_z^2} - \frac{p_x^2}{2\,p_z^2} - \frac{p_y^2}{2\,p_z^2} - \frac{p_y}{p_z^2}A\,sin(\zeta) \ , \tag{9}$$

$$\frac{dp_z}{d\tau} = -\,k_z\frac{p_y}{p_z}A\,cos(\zeta) \ , \tag{10}$$

where the normalized time coordinate $\tau = ct$. The $y$-motion consists of an oscillation in the ion channel potential, subject to the Lorentz force due to the signal field,

$$\frac{dy}{d\tau} = \frac{p_y}{p_z} + \frac{A}{p_z} sin(\zeta) , \tag{11}$$

$$\frac{dp_y}{d\tau} = -\frac{1}{2} k_p^2 y , \tag{12}$$

and coupled to the $z$ motion via $p_z$ and $A$. The $x$-motion is a free oscillation in the potential well, which is however coupled to the axial motion via $p_z$ due to the relativistic mass effect,

$$\frac{dx}{d\tau} = \frac{p_x}{p_z} , \tag{13}$$

$$\frac{dp_x}{d\tau} = -\frac{1}{2} k_p^2 x . \tag{14}$$

In Eqs. (9)-(14), derivatives of the slowly varying eikonal quantities, and their transverse gradients, have been neglected.

The particle motion simplifies with an average over the rapid betatron motion. For this purpose, the transverse momenta may be expressed in terms of eikonal variables $q_x$, $q_y$, $\theta_y$, and $\theta_y$, such that

$$p_x = q_x sin(\theta_x) , \tag{15}$$

$$p_y = q_y sin(\theta_y) , \tag{16}$$

For $A=0$, $q_x$ and $q_y$ are constants and $d\theta_{x,y}/d\tau = k_\beta = \omega_\beta / c$. With averaging, Eqs. (9) and (10) become

$$\overline{\frac{dz}{d\tau}} = 1 - \frac{1}{2q_z^2} - \frac{q_x^2}{4q_z^2} - \frac{q_y^2}{4q_z^2} + \frac{1}{2}\frac{q_y}{q_z^2}A\cos(\psi)\,, \tag{17}$$

$$\overline{\frac{dq_z}{d\tau}} = -\frac{1}{2}k_z c\frac{q_y}{q_z}A\sin(\psi)\,, \tag{18}$$

where the bar indicates the average over the betatron period. In deriving Eqs. (17) and (18) we neglected axial oscillations in $z$ at frequency $2\omega_\beta$, which occur as an electron climbs or descends the ion-channel potential. Neglect of this "jitter" is appropriate in the limit $q_x, q_y \ll 1$. In addition, it is assumed that the phase of the transverse motion measured with respect to the phase of the radiation field and averaged over the betatron period,

$$\psi = \theta_y + \bar{\zeta} \tag{19}$$

is slowly varying on the scale $k_\beta^{-1}$. This condition requires that the "detuning" parameter

$$\Omega = k_z\,\bar{\beta}_z - \frac{\omega}{c} + k_\beta\,, \tag{20}$$

be small compared to $k_\beta$. The quantity

$$\bar{\beta}_z = 1 - \frac{2 + q_x^2 + q_y^2}{4p_z^2} = 1 - \frac{1 + p_z H_\perp}{2p_z^2}\,, \tag{21}$$

is the normalized drift velocity in $z$, at zeroth order, averaged over the betatron period. Note that detuning depends only on $p_z$ and $H_\perp$,

not $q_x$ or $q_y$ individually. For example, a step radial profile and a monoenergetic beam, corresponds to a delta function distribution in $H_\perp$ and $p_z$, and there is no spread in $\Omega$.

To average Eqs. (11)-(14) we differentiate, eliminating $x$ and $y$,

$$\frac{d^2 p_x}{d\tau^2} + k_\beta^2 p_x = 0 \ , \tag{22}$$

$$\frac{d^2 p_y}{d\tau^2} + k_\beta^2 p_y = - k_\beta^2 A \sin(\zeta) \ . \tag{23}$$

At first order in $A$, these equations, expressed in terms of eikonal variables, reduce to

$$\frac{d\theta_x}{d\tau} = k_\beta \ , \tag{24}$$

$$\frac{d q_x}{d\tau} = - \frac{q_x}{2 k_\beta} \frac{d k_\beta}{d\tau} \ , \tag{25}$$

$$\frac{d\theta_y}{d\tau} = k_\beta \left( 1 - \frac{A}{2 q_y} \cos(\psi) \right) , \tag{26}$$

$$\frac{d q_y}{d\tau} = - \frac{q_y}{2 k_\beta} \frac{d k_\beta}{d\tau} - \frac{1}{2} k_\beta A \sin(\psi) \ , \tag{27}$$

and formally $q_y > O(A)$ is assumed in Eq. (26). This approximation is valid even in the limit $q_y \rightarrow 0$, since all terms varying as $1/q_y$ are eventually multiplied by $q_y$, *i.e.*, $q_y exp(i\theta_y)$, is always well-defined, even if the phase is varying rapidly. The formal divergence at $q_y \rightarrow 0$ simply shows that an initially small transverse oscillation adjusts rapidly to a phase determined by the wave, independent of $q_y(0)$

and $\theta_y(0)$. In these equations the terms involving $dk_\beta/d\tau$ contribute at higher order in $q_x$, $q_y$ and may be neglected.

Combining these results and eliminating $z$ in favor of $\psi$, the equations of motion take a form reminiscent of that found by Kroll, *et al.*, for the free-electron laser (FEL),[9]

$$\frac{d\psi}{d\tau} = k_z \bar{\beta}_z - \frac{\omega}{c} + \frac{d\theta_y}{d\tau} + \frac{d\varphi}{d\tau} + \frac{1}{2} k_z \frac{q_y}{p_z^2} A \cos(\psi) , \tag{28}$$

$$\frac{d\theta_y}{d\tau} = k_\beta \left( 1 - \frac{1}{2 q_y} A \cos(\psi) \right), \tag{29}$$

$$\frac{dp_z}{d\tau} = -\frac{1}{2} k_z \frac{q_y}{p_z} A \sin(\psi) , \tag{30}$$

$$\frac{dq_y}{d\tau} = -\frac{1}{2} k_\beta A \sin(\psi) . \tag{31}$$

Note that the formal singularity in Eq. (29) may be removed by replacing the variables $\theta_y$ and $q_y$ with the complex variable,

$$X = q_y \exp(-i\chi) , \tag{32}$$

where $\chi=\psi-\varphi$.

Equations (28)-(31) show that $\psi$ determines the sign and magnitude of all the perturbative effects of the field. From Eq. (28) it is evident that the evolution of $\psi$ is dominated by variations in $\bar{\beta}_z$ and $\theta_y$, which are in turn determined by the variations in $p_z$ and $q_y$. For a fast-wave ($\omega \sim ck_z$) Eq. (30) describes the slowing of particles with $\psi>0$ and the acceleration of particles with $\psi<0$, due to the $z$-component of the Lorentz force, *i.e.*, the ponderomotive force. The

first term on the right in Eq. (31), as well as the first-order term in Eq. (29), are due to the $y$-component of the Lorentz force. These terms arise from the resonant perturbation of the transverse motion. In an FEL this effect is small; here, it will be non-negligible.

To gain further insight into Eqs. (28)-(31), consider the motion of a "test" particle. Combining Eqs. (28) and (29) yields

$$\frac{d\psi}{d\tau} = \frac{d\varphi}{d\tau} + \Omega - \Pi A \cos(\psi) , \tag{33}$$

where the parameter $\Pi$ is

$$\Pi \approx \frac{k_\beta}{2 q_y} , \tag{34}$$

and arises from the $q_y$ variation of Eq. (29). Equation (33) shows that particles with small $q_y$ can be significantly detuned from resonance. This is because the phase of a driven harmonic oscillator varies rapidly when its initial amplitude is small.

Examining Eq. (33) it is tempting to think of $\Omega > 0$ as corresponding to a particle with energy above resonance, as in an FEL. However, from Eq. (20), $\Omega$ depends on both $\bar{\beta}_z$, (which increases with $p_z$) and $k_\beta$, which decreases with $p_z$. Thus higher energy particles drift faster in $z$, but they oscillate more slowly. Depending on the wave phase velocity, more energetic particles may actually be below resonance.

To make this more precise, we differentiate Eq. (33) and subsititute from Eqs. (28)-(32), to obtain,

$$\frac{d^2\psi}{d\tau^2} \approx -\left\{\Xi - \Pi\frac{d\psi}{d\tau}\right\} A\, sin(\psi) - \Pi\frac{dA}{d\tau}\, cos(\psi) \quad , \tag{35}$$

where the bunching parameter $\Xi$ is

$$\Xi \approx \frac{k_z^2}{2\, p_z^4} q_y \left\{1 - \frac{k_\beta}{k_z} p_z^2\right\} . \tag{36}$$

This parameter describes the dependence of detuning on energy, and includes a negative (antibunching) term due to the relativistic mass effect, and the $y$-component of the Lorentz force. In the slow-wave limit ($k_z c < \omega$), the relativistic mass effect and transverse damping dominate bunching, which occurs in the opposite sense as for axial bunching. An analogous transition in bunching was examined by Chu and Hirshfield[10] for the cyclotron maser instability. Here, the transition ($\Xi$=0) occurs for $k_z \sim k_\beta p_z^2$, which corresponds to a group velocity close to $c\bar{\beta}_z$. Thus $\Xi$ varies from a value which is appreciable (for $\omega = k_z c$, $\Xi \sim k_\beta^2 q_y$), to zero over a small range of phase velocity $1 < \beta_\varphi < 1 + 1/2p_z^2$, where $\beta_\varphi = \omega/ck_z$.

The effect of the $\Xi$-term is clarified by considering motion in a constant eikonal, for which Eq. (35) simplifies to

$$\frac{d^2\psi}{d\tau^2} \approx -\Xi A\, sin(\psi) \quad , \tag{37}$$

and $|\Xi| >> \Pi d\psi/dt$ is assumed, corresponding to an appreciable value of $q_y$. Thus $\psi$ oscillates as in a nonlinear pendulum with stable point $\psi \sim 0$

($\psi \sim \pi$) for $\Xi>0$ ($\Xi<0$). In a growing eikonal Eq. (37) describes bunching about the stable point, corresponding to the growth of a beam centroid oscillation coherent with the signal.

Further insight into Eqs. (28)-(31) is gained by considering the constants of the motion,

$$\Phi_x = J_x \,, \tag{38}$$

$$\Phi_y = J_y - \frac{H}{\omega} \,, \tag{39}$$

$$\Phi_z = \frac{H}{\omega} - \frac{p_z}{c\,k_z} \,. \tag{40}$$

Here $J_x$ and $J_y$ are the invariant actions of the unperturbed motion. Equation (39) defines a modified action for the $y$-motion, and shows that a loss of energy $\Delta H$ is accompanied by a loss of action in amount $\Delta H/\omega$. This result is consistent with Liouville's theorem, given the coupling to the $z$-motion, and can be adduced to demonstrate the stability of a beam with negligible transverse energy. The quantity $\Phi_z$ of Eq. (40) is constant since energy $\Delta H$ deposited in the fields will correspond to a field momentum $\Delta p_z=(k_z c/\omega)\Delta H$, and this axial impulse must be taken up by the particles, in the absence of external axial forces.

These invariants are helpful in understanding the bunching parameter, $\Xi$. A loss of axial momentum is compensated in part by a loss of transverse energy, due to the relativistic mass effect and the resonant damping of the transverse motion. When $k_z \sim k\beta p_z^2$, these effects cancel and $\Xi$ vanishes; bunching is stationary with respect to variations in axial momentum, brought about by interaction with the

eikonal. With three integrals of the motion in hand, one may in principle describe the particle motion with just two equations, for $p_z$ and $\psi$, analogous to those for the FEL.

## C. Maxwell's equations

Having examined the single-particle motion, consider next the feedback from an ensemble of such particles, through the field equations. Maxwell's equations are

$$\left\{\nabla_\perp^2 + \frac{\partial^2}{\partial z^2} - \frac{1}{c^2}\frac{\partial^2}{\partial t^2}\right\} A_y = -\frac{4\pi}{c} J_y \,, \tag{41}$$

where $A_y$ is the vector potential in the Lorentz gauge, $J_y$ is the transverse beam current density, and $\nabla_\perp^2$ is the Laplacian in the transverse plane. The high-frequency scalar and axial vector potentials ("space-charge effects") have been neglected. The radial mode is assumed to be specified, corresponding to a transverse wavenumber $k_\perp$, satisfying $k_\perp a \ll 1$, where $a$ is the beam radius. We define the mode area, $\Sigma$

$$\Sigma^{-1} = \frac{|A_y(r=0)|^2}{\int dx\,dy\,|A_y|^2} \,, \tag{42}$$

the overlap integral $\eta = \pi a^2/\Sigma$, and $\omega$ is assumed to satisfy the dispersion relation,

$$\omega^2 = c^2(k_z^2 + k_\perp^2) \,. \tag{43}$$

Expressing $A_y$ in terms of the eikonal quantities $A$ and $\varphi$, from Eqs. (2) and (3), and neglecting second derivatives, and products of derivatives, of $A$ and $\varphi$, Eq. (41) reduces to

$$\left\{ k_z \frac{\partial}{\partial z} + \frac{\omega}{c}\frac{\partial}{\partial \tau} + i\frac{\omega_{beff}^2}{2\,c^2}\left\langle \frac{1}{p_z} \right\rangle \right\} (A\,e^{i\varphi}) = i\,\frac{\omega_{beff}^2}{2\,c^2}\left\langle \frac{q_y}{p_z}\,exp(-i\chi) \right\rangle, \tag{44}$$

where the effective beam plasma frequency is given by

$$\omega_{beff}^2 = \frac{4\,\pi\,c^2}{\Sigma}\left(\frac{I}{I_o}\right), \tag{45}$$

and $\chi=\psi-\varphi$. In this expression, an average has been performed over the period $2\pi/\omega$ and over all electrons at $z,t$, as indicated by the brackets. Following essentially the treatment of Bonifacio, *et al.*, for the FEL,[11] we will neglect "slippage", assuming that the eikonal group velocity is close to the average beam axial velocity $V$. In terms of the $\tau$-derivative at fixed $s=Vt-z$, Eq. (45) then reduces to,

$$\frac{\partial A}{\partial \tau} = \frac{\omega_{beff}^2}{2\,\omega c}\left\langle \frac{q_y}{p_z}\,sin(\psi) \right\rangle, \tag{46}$$

$$\frac{\partial \varphi}{\partial \tau} = -\,\nu + \frac{1}{A}\frac{\omega_{beff}^2}{2\,\omega c}\left\langle \frac{q_y}{p_z}\,cos(\psi) \right\rangle, \tag{47}$$

where

$$\nu = \frac{\omega_{beff}^2}{2\,c\,\omega}\left\langle \frac{1}{p_z} \right\rangle, \tag{48}$$

represents the shift in frequency due to the non-resonant portion of the beam susceptibility. Equations (46), (47) and (28)-(32) are the basic equations describing the "ion-channel laser" instability.

Note that the power associated with a drifting beam slice and the comoving eikonal wave front

$$P \approx mc^2 I \langle H - 1 \rangle + \frac{1}{8\pi} P_0 \Sigma \left(\frac{\omega}{c}\right)^2 A^2 , \tag{49}$$

is constant in $\tau$. Here $P_0 = m^2c^5/e^2 \sim 8.7$ GW.

## D. Dispersion relation

To examine linear amplification, we may rewrite Eqs. (46) and (47) in terms of the complex eikonal $B = Ae^{i\varphi}$,

$$\left(\frac{\partial}{\partial\tau} + iv\right)B = i\,\frac{\omega_{beff}^2}{2\,\omega c}\left\langle \frac{q_y}{p_z} exp(-i\chi) \right\rangle . \tag{50}$$

Expanding $\chi = \chi_0 + \chi_1$ and $q_y = q_{y0} + q_{y1}$ in zeroth and first order terms gives

$$\left(\frac{\partial}{\partial\tau} + iv\right)B \approx \frac{\omega_{beff}^2}{2\,\omega c}\left\langle exp(-i\chi_0)\left(\frac{q_{y0}}{p_z}\chi_1 + i\frac{q_{y1}}{p_z}\right)\right\rangle . \tag{51}$$

(In principle, there is also a perturbed $p_z$ term, but it contributes at higher order in $q_y^2$.) The perturbed phase is determined from Eqs. (28)-(32), or equivalently, Eq. (35),

$$\frac{d^2\chi_1}{d\tau^2} = -\left\{\Xi - \Pi\left(\frac{d\chi_0}{d\tau} + \frac{d\varphi}{d\tau}\right)\right\} A\, sin(\chi_0 + \varphi) - \Pi\frac{dA}{d\tau} cos(\chi_0 + \varphi) \tag{52}$$

Writing $\chi_1 = Im(\tilde{\chi}_1)$ , we have

$$\frac{d^2\tilde{\chi}_1}{d\tau^2} = -\Xi B e^{i\chi_0} - i\Pi\frac{d}{d\tau}\left(B e^{i\chi_0}\right). \tag{53}$$

We look for a solution $B(t) \propto exp(\Gamma\tau)$, and integrate Eq. (53) to obtain

$$\tilde{\chi}_1 \approx -\left\{\frac{\Xi}{(\Gamma + i\Omega)^2} + \frac{i\Pi}{(\Gamma + i\Omega)}\right\} B e^{i\chi_0}, \tag{54}$$

neglecting small constants of integration.

The $q_{y1}$ term in Eq. (51) is obtained by linearizing Eq. (31),

$$\frac{dq_{y1}}{d\tau} \approx -\frac{1}{2} k_\beta A\, sin(\chi_0 + \varphi), \tag{55}$$

which is integrated to give

$$q_{y1} \approx -\Im\left\{\frac{q_{y0}\,\Pi}{(\Gamma + i\Omega)} B e^{i\chi_0}\right\}, \tag{56}$$

neglecting small constants of integraton.

Combining Eqs. (51), (54) and (56) results in the dispersion relation

$$\Gamma + i\nu = i\frac{\omega_{beff}^2}{4\,\omega c}\left\langle \frac{q_y}{p_z}\left\{\frac{\Xi}{(\Gamma + i\Omega)^2} + \frac{2\,i\Pi}{(\Gamma + i\Omega)}\right\}\right\rangle . \tag{57}$$

## III. ANALYSIS OF THE DISPERSION RELATION

### A. "Cold" Beam (uniform detuning)

The simplest limit of Eq. (57) corresponds to a detuning $\Omega$ which is the same for each particle. In this case, the resonant denominators may be removed from the average. Defining a dimensionless parameter $\zeta$, and detuning $\delta$,

$$\zeta = (i\Gamma - \Omega) / k_\beta , \tag{58}$$

$$\delta = (\Omega - \nu) / k_\beta , \tag{59}$$

the dispersion relation takes the form

$$\zeta^3 + \delta\zeta^2 - \mu^2\,\zeta - 8\,\rho^3 = 0 . \tag{60}$$

The gain parameter $\rho$ is given by

$$\rho^3 = \frac{\omega_{beff}^2}{32\,\omega k_\beta^3 c}\left\langle \frac{q_y}{p_z}\,\Xi\right\rangle = \left(\frac{\eta I}{32\,p_z I_0}\right)\vartheta(\beta_\varphi, p_z)^3 , \tag{61}$$

where the function $\vartheta$=1 for a fast-wave, and for $\beta_\varphi \neq 1$,

$$\vartheta(\beta_\varphi, p_z) \approx \left\{ \frac{1 - 2\,p_z^2(\beta_\varphi - 1)}{1 + 2\,p_z^2(\beta_\varphi - 1)} \frac{1}{\beta_\varphi} \right\}^{1/3}, \tag{62}$$

taking $\beta_z \sim 1 - 1/2p_z^2$, and neglecting $\Omega$. This variation of the gain parameter with wave phase velocity may be understood from the discussion of Eq. (36). For definiteness we will assume $\rho>0$; from the symmetry of Eq. (60) this entails no loss of generality.

The constant $\mu$ is given by

$$\mu^2 = \frac{\omega_{beff}^2}{2\,\omega k_\beta^2 c} \left\langle \Pi \frac{q_y}{p_z} \right\rangle \approx 8 \frac{\rho^3}{a_\beta^2}, \tag{63}$$

and the last equality holds in the fast-wave limit. The dimensionless parameter $a_\beta$ is given by

$$a_\beta^2 = \langle q_y^2 \rangle = \langle p_z H_\perp \rangle, \tag{64}$$

and plays a role simliar to that of the "wiggler parameter" in an FEL. Note that the assumption $q_x, q_y \ll 1$, requires $a_\beta^2 \ll 1$. In evaluating the averages in Eqs. (61), (63) and (64) we have assumed a step radial profile, for which $a_\beta = p_z k_\beta a/2^{1/2}$.

Considerable insight is gained by comparison of Eq. (60) with the FEL dispersion relation in the limit of small "wiggler" parameter, with a uniform distribution in detuning.[12] In fact, it is not hard to show that the two dispersion relations are identical, if one identifies (1) $k_\beta$ with the FEL wiggler wavenumber, (2) $\rho$ with the FEL Pierce

parameter and (3) $\pm\mu k_\beta$ with the FEL detuning spread. Thus a number of results from FEL theory may be taken over directly.

In general, the solution for the eikonal is a superposition of three terms corresponding to the three roots $\zeta_\pm$, $\zeta_0$, of Eq. (60), at most one of which, $\zeta_+$ results in amplification. The solution for the normalized growth rate $Im(\zeta_+)$ is depicted in Fig. 3. For illustration, consider the limit $\delta,\mu<<\rho$, in which Eq. (60) reduces to a simple cubic. In this "cubic gain regime" the signal is amplified with exponential gain length, $L_g\sim\beta_z/Re(\Gamma_+)$, where $Re(\Gamma)=k_\beta Im(\zeta_+)$, so that

$$L_g = \frac{\lambda_\beta}{2\,\pi 3^{1/2}\,\rho} \approx 0.3\,\lambda_\beta \left(\frac{\gamma I_0}{\eta I}\right)^{1/3}, \tag{65}$$

with $\lambda_\beta\sim 2\pi\beta_z/k_\beta$ the betatron period. Depending on current, energy and the overlap factor, this gain length may be as short as a few betatron wavelengths. Efficiency may be estimated by taking $\chi_I\sim O(1)$, corresponding to the onset of non-linearity and particle trapping, This gives an efficiency of $\sim\rho$, and and output power $P_{sat}\sim\rho P_{beam}$, where $P_{beam}\sim mc^2(\gamma-1)I$ is the initial beam power. A rough estimate of the length for saturation is $L_{sat}\sim 0.5L_g ln(9P_{sat}/P_i)$, where $P_i$ is the input power.[13]

Generally, these $\mu=\delta=0$ results are useful for simple estimates of instability growth. However, they represent the optimal performance possible and the approximation $\mu=0$ omits some important features. In particular, without special preparation a typical beam will have a spread in transverse energy, corresponding to a detuning spread of order $k_\beta a_\beta^2$. If $\mu$ is small, this detuning spread is large, and gain will

be reduced. Thus the finite $\mu$ limit is of intrinsic interest (moreso than for the FEL).

In general, the instability is stabilized for a finite positive detuning, which for $\mu=0$ is $\delta/\rho\sim3.8$. As $\mu/\rho$ increases to $\mu/\rho\sim2.8$, this upper bound on $\delta$ decreases to 0. On the other hand, for any finite negative detuning, there is some range of $\mu$ which yields growth. Conversely, for any $\mu$, there is some negative detuning which yields growth (provided $|\delta|<<1$). Practically, for a given $\mu$, it is useful to have in hand the maximum growth rate, as depicted in Fig. 4(a), with the corresponding detuning in Fig. 4(b).

It is also useful to have analytic formulas, for the limit $|\delta|>>\mu,\rho$, with $\delta<0$. In this limit, as for the FEL, the growing root is the solution of a quadratic ("quadratic gain regime"),

$$\zeta_0 \approx -\delta - \frac{\mu^2}{\delta}, \tag{66}$$

$$\zeta_\pm \approx \frac{\mu^2 \pm \sqrt{32\,\rho^3\,\delta + \mu^4}}{2\,\delta}, \tag{67}$$

and the threshold for gain in this limit is $\rho^3\delta<-\mu^4/32$. Far above threshold, $Im(\zeta_+)$ decreases slowly, as $1/|\delta|^{1/2}$, as seen in Fig. 3. From Eq. (67) the maximum growth rate occurs at $\delta\sim-4\rho^3/a_\beta^4$, and corresponds to $\zeta_+\approx 8\,\rho^3(-1+i)/\mu^2$. In the limit $a_\beta^2<<\rho$, the peak growth rate is $Im(\zeta_+)\sim a_\beta^2$.

To summarize, the detuning effect represented by the $\mu$ term in Eq. (60) (or the $\Pi$ term in Eqs. (33) or (57)) tends to reduce growth, even eliminating growth for some range of $\delta$ and $\rho$. We have seen

that the competition between the bunching ($\Xi$) and antibunching ($\Pi$) terms depends on the ratio $\rho/a_\beta^2$. It also depends on detuning, since the ponderomotive force may be varied by tuning the beam off-resonance.

## B. Effect of Detuning Spread

Next consider the effect of a spread in $\Omega$. We define the dimensionless center detuning $\delta_0 = <\Omega - v>/k_\beta$, and introduce a new particle variable $\delta_1 = (\Omega - <\Omega>)/k_\beta$. In terms of $\zeta$ defined by $\zeta = <i\Gamma - \Omega>/k_\beta$, the dispersion relation takes the form

$$\zeta + \delta_0 = \mu^2 \left\langle \frac{1}{(\zeta + \delta_1)} \right\rangle + 8\ \rho^3 \left\langle \frac{1}{(\zeta + \delta_1)^2} \right\rangle . \tag{68}$$

The effect of momentum spread may be modelled by taking particles to be uniformly distributed over some range of detuning $-\delta_s < \delta_1 < \delta_s$. The dispersion relation then becomes,

$$\zeta + \delta_0 = \frac{\mu^2}{2\ \delta_s}\ ln\left(\frac{\zeta + \delta_s}{\zeta - \delta_s}\right) + \frac{8\ \rho^3}{\zeta^2 - \delta_s^2} . \tag{69}$$

It is straightforward to show that in the limit of large $\delta_s$, the roots are real, corresponding to stabilization. In the limit of small $\delta_s$, Eq. (69) takes the approximate form

$$\zeta^3 + \delta\zeta^2 - (\ \mu^2 + \delta_s^2\ )\ \zeta - 8\ \rho^3 \approx 0 , \tag{70}$$

and is formally identical to Eq. (60) provided we make the replacement $\mu \rightarrow \hat{\mu} = (\mu^2 + \delta_s^2)^{1/2}$. Thus the discussion and conclusions for the cold beam case may be carried over directly.

The resulting conditions for gain, expressed in terms of $\delta_s$ may be related to practical constraints on the beam through the dependence of detuning on $p_z$ and $H_\perp$ as given by Eq. (21). In the fast-wave limit this gives $\delta_s \sim 1.5 p_s/p_z$ for a momentum spread of $\pm p_s$. For a spread in transverse energy $\pm h_s$, $\delta_s \sim p_z h_s$. In principle there are four sources of detuning spread in the IFR. The first is detuning spread due to a spread in beam energy. In addition, from Eq. (7), there is a momentum spread of order $p_s/p_z \sim \sigma_1 v/p_z$. While for typical beam profiles, there is a spread in $H_\perp$, $h_s \sim \sigma_2 a_\beta^2/p_z$. Moreover, due to beam self-fields there is a spread in $k_\beta$ corresponding to a detuning spread, $\delta_s \sim \sigma_3 v/p_z a_\beta^2$. The dimensionless quantities $\sigma_i < 1$ are factors depending on the beam profile. For a step profile, $\sigma_i = 0$. For estimates we will take $\sigma_i \sim 0.5$.

## C. Discussion

Having exploited the similarities with the FEL it is important to note a significant *difference*. Bunching in the phase $\psi$ does not correspond to a simple axial resolution of the beam into a stream of charge bunches separated by a signal wavelength, as in an FEL. Instead the centroid oscillations of a beam slice become coherent, as discussed in connection with Eq. (37). To check this, one may simply calculate the average $y$-momentum in a beam slice from the linearized equations of motion. In the small $\mu$ limit, for $z >> L_g$, this is,

$$\langle p_y \rangle \approx -\frac{1}{2^4}\frac{a_\beta^2}{\rho^2} A \sin( k_z z - \omega t + \varphi + \frac{2\pi}{3}) \quad . \tag{71}$$

Thus amplification of the eikonal proceeds by feedback in the form of growing beam centroid oscillations. This feature has motivated analogies with the cyclotron auto-resonant maser.[6]

Further insight into the mechanism of amplification is revealed by examining the ponderomotive force. In the fast-wave limit and expressed in terms of $\zeta_r = Re(\zeta_+)$ and $\zeta_i = Im(\zeta_+)$, this takes the form

$$\left\langle \frac{dH}{d\tau} \right\rangle \approx \frac{1}{4\, p_z}\frac{\omega}{c} A^2 \left\{ 2\, a_\beta^2 \frac{\zeta_r \zeta_i}{(\zeta_r^2 + \zeta_i^2)^2} + \frac{\zeta_i}{(\zeta_r^2 + \zeta_i^2)} \right\} . \tag{72}$$

Thus for a beam with negligible transverse energy ($a_\beta^2 \rightarrow 0$), $dH/d\tau$ and $\zeta_i$ are of the same sign. Energy conservation then implies that growth vanishes ($\zeta_i \rightarrow 0$) in this limit, confirming that an ensemble of simple harmonic oscillators with negligible transverse energy is stable against electromagnetic perturbations. This also shows that that when $\rho > 0$ (*i.e.*, when electrons bunch about $\psi \sim 0$), gain requires $-k_\beta \zeta_r \sim d\varphi/d\tau + \Omega > 0$.[14] This can also be understood from Eq. (33), and occurs because particles are being continually detuned from resonance by the transverse Lorentz force, with a sign depending on the wave phase velocity.

Said differently, the driven transverse velocity in an eikonal of constant amplitude is ninety degrees out of phase with the electric field, as reflected in the factor of $i$ multiplying $\Pi$ in Eq. (57). Thus no

net work is performed on the fields, on average. On the other hand, when the eikonal is growing, the driven motion absorbs energy from the wave, while the "free" oscillation does work on the fields, mediated by axial bunching. If there is no free oscillation ($a_\beta^2 \to 0$), the system is stable.

## IV. EXAMPLE

To test the analytic results of Sec. III, we consider a specific example with parameters as given in Table I, corresponding to a microwave amplifier, operated in the $TE_{10}$ mode of rectangular waveguide. The beam parameters for this example correspond roughly to what has already been achieved with induction accelerators.[15]

### A. Analytic estimates

For a free-space wavelength $\lambda \sim 3.2$ cm ($\omega/2\pi \sim 9.4$ GHz), and 5.5cmx11cm guide, resonance corresponds to a betatron wavelength $\lambda_\beta \sim 30$cm and a plasma density $n_p \sim 5 \times 10^{12}$ cm$^{-3}$. The transverse wavenumber is $k_\perp = \pi/w_x \sim 0.3$ cm$^{-1}$, so that $k_z \sim 1.9$cm$^{-1}$, from Eq. (43). The phase velocity is $\beta_\varphi \sim 1.01$, and $p_z \sim 2.7$, corresponding to a reduction in the Pierce parameter by a factor $\vartheta \sim 0.9$, from Eq. (62). The mode area is $\Sigma = w_x w_y/2 \sim 30\text{cm}^2$, corresponding to an overlap factor $\eta = 2\pi a^2/w_x w_y \sim 0.2$. The Pierce parameter is $\rho \sim 7.4\%$, from Eq. (61). From Eq. (65) one expects a gain length of $L_g \sim 0.1\lambda_\beta/\rho \sim 40$ cm, corresponding to a gain of 22dB/m. Assuming an input power $P_0 \sim 50$

kW, the cubic gain regime scalings predict saturation in a length $L_{sat}$~2.7m, with power at saturation $P_{sat}$~2.9x10$^8$W. On the other hand, $a_\beta^2$~0.5, so that $\mu/\rho$~1.4 and, from Fig. 4(a), one may expect somewhat lower gain and peak power.

## B. Numerical results

To check these analytic predictions, we follow instability growth numerically, using two codes, ECL and FCL. The code ECL solves the betatron-averaged equations, Eqs. (28)-(31), expressed in terms of the variable $X$ of Eq. (32), combined with Maxwell's equations, Eq. (50). The code FCL solves the full equations of motion, Eqs. (9)-(14) and Maxwell's equations, Eq. (50), with the eikonal average removed.

As seen in Fig. 5, ECL predicts $P_{sat}$~ 2.2x10$^8$W, with saturation in a length $L_{sat}$~2.8 m, for an efficiency of 5.6%. FCL is in rough agreement, predicting $P_{sat}$~2.3x10$^8$W, with saturation in a length $L_{sat}$~3.0 m. for an efficiency of 5.8%. Note that the deviations from simple exponential growth in Fig. 5 arise from the detuning $\nu$ of Eq. (48), the effective detuning spread $\mu$ of Eq. (63), and the presence of all three roots of Eq. (60) in the numerical solution. Figure 6 depicts the FCL results for $y$-momentum averaged over the ensemble and rms normalized emittance in $y$. The maximum momentum amplitude $<p_y>$~0.3 is roughly the value $<p_y>\sim a_\beta/2^{3/2}$~0.2 predicted by Eq. (66). The fractional reduction in rms $y$-emittance may be estimated from Eq. (39), $\Delta\varepsilon_{ny}/\varepsilon_{ny}\sim \rho/a_\beta^2\sim$ 0.3 and agrees well with the numerical result.

Next consider finite temperature effects. The spread in momentum due to self-fields will be of order $\nu/2p_z$~5%, while that

due to a typical spread in transverse energy will be of order $a_\beta^2/2 \sim 10\%$. The effect of detuning spread on gain as predicted by ECL is summarized in Fig. 7. Evidently, a detuning spread $\delta_s < \rho$ has only a small effect on output power (about a factor of two), in accord with the results of Sec. III.

On the other hand, Fig. 4 predicts that optimal gain requires a negative detuning. This motivates a survey of $P_{sat}$ versus $\delta_0$ at fixed $\delta_s$, as depicted in Fig. 8. Thus, for example, with $\delta_0 \sim 0$ and $\delta_s \sim 15\% \sim 2\rho$, peak power is $P_{sat} \sim 1 \times 10^7$W. However, for $\delta_0 \sim -20\%$, $P_{sat} \sim 7 \times 10^7$W, only a factor of three reduced from the $\delta_s = 0$ result.

To check the effect of nonlinear focussing we consider a gaussian radial ion profile $\propto exp(-r^2/b^2)$, with waist $b$ equal to the beam radius, $a \sim 1.4$ cm. The code FCL predicts saturation in a length $L_{sat} \sim 2.7$m, with peak power $P_{sat} \sim 1.9 \times 10^8$W. This implies that the naive estimate of detuning spread due to beam self-fields $\delta_s \sim \nu/2p_z a_\beta^2 \sim 16\%$ is somewhat of an overestimate.

In addition, one should consider plasma effects deleterious to gain. The chief constraint is due to ion-motion and imposes a limit on the pulse length. The ion-neutralization time-scale is $2\pi/\omega_i \sim 250$ ns, assuming a molecular weight of ~150 amu as for diethlyaniline. The slosh time-scale is $2\pi/\omega_s \sim 160$ ns. These time-scales are acceptable, considering that induction linacs provide pulse lengths in the range 10 ns - 100's of ns. The ion-hose growth length computed in the rigid beam model[2] for a 20 ns pulse is $L_h \sim 8$ cm, with about four e-folds after three meters. As for other plasma effects, emittance growth due

to scattering is negligible[16,17] as are the beam-ion longitudinal two-stream instability,[2] and beam head erosion.[18]

In summary, the numerical results of this section have confirmed the scaling laws for efficiency, gain length, and saturated power. For the example presented, amplification would be observable and the parameters appear practical for a proof-of-principle experiment.

## V. CONCLUSIONS

A simple formulation for an electromagnetic instability of the ion-focused regime has been presented. It has been shown that the Pierce parameter $\rho$ roughly determines the efficiency and the gain length. It was also shown that corrections due to detuning spread may be crucial depending on the parameters. A practical conclusion from this work is that control of such detuning spread will be vital to a successful experiment. (At the same time note that a method of conditioning beams to effectively remove such an axial velocity spread has recently been proposed.[19])

Analytic scaling laws were verified via numerical simulation for a particular example and it was shown that, for reasonable beam and plasma parameters, amplification would be observable. Indeed such a microwave "ion-channel laser" could achieve performance comparable to that of an FEL, without the expense of magnets and magnet power supplies.

To place these results in context, one may view the ion-channel laser as simply another fast-wave free-electron device; the similarity with the FEL, and the differences, are discussed in connection with Eqs. (60) and (71). One may also draw analogies with the quadrupole FEL proposed by Levush, *et al*,[20] work of Latham,[21] and more recent work by Tang, *et al.*[22] One expects a similar betatron-coupled instability in the magnetically self-focussed regime of propagation, and this appears to have been observed experimentally.[23,24] Theoretical work for this regime also has been performed.[25]

This work suggests a number of areas for further research, one of which is radiation guiding. The original guiding mechanism proposed in Ref. 5, ion-channel dielectric guiding, now appears problematic due to the electron-hose instability.[26] However, one expects optical guiding, as in an FEL, due to the resonant contribution to the radially varying dielectric constant.[27,28,29] The simple treatment of this effect given in Ref. 7, indicates that optical guiding is typically quite strong and a thorough analysis of the strong-guiding limit may well reveal the possibility of producing intense, short-wavelength (microns to nanonmeters) radiation with high efficiency. A particular attraction of the IFR at such wavelengths is that in a plasma, $\lambda_\beta$ may be exceedingly small compared to a typical FEL wiggler period. This permits operation at a lower energy (and higher efficiency) for a given wavelength. Practically, guiding itself is readily amenable to experimental tests; for example, for the parameters of Table I the optical guiding overlap is predicted to be of order unity, corresponding to a reduction by a factor of two both in gain length and the detuning spread constraint.

Another subject of interest is the ion slosh motion, which could give rise to an electromagnetically coupled ion-hose instability, and result in emittance growth toward the tail of a long pulse, even when the initial beam alignment is "perfect".

## ACKNOWLEDGMENTS

Discussions and joint efforts with John M. Dawson and Andrew M. Sessler were invaluable. This work also owes much to thoughtful comments from William A. Barletta, Kuan-Ren Chen, Shigenori Hiramatsu, Thomas Katsouleas, Baruch Levush, Ernst T. Scharlemann, Gennady Shvets, Ken Takayama, and Jonathan S. Wurtele.

Work at LBL was supported by the Office of Energy Research, U.S. Dept. of Energy, under Contract No. DE-AC03-76SF00098. Work in Japan was supported by the XIV International Conference on High Energy Accelerators, the National Laboratory for High Energy Physics (KEK), and a postodoctoral award from the Japan Society for the Promotion of Science, in cooperation with the National Science Foundation.

[a] Present address: Accelerator Division, National Laboratory for High Energy Physics, 1-1 Oho, Tsukuba, Ibaraki, 305, Japan.

[1]G. I. Budker, *Proceedings of the CERN Symposium on High Energy Accelerators and Pion Physics*, (Geneva, 1956) pp. 68-75.

[2] H. L. Buchanan, Phys. Fluids **30**, 221 (1987).

[3]G. J. Caporaso, F. Rainer, W. E. Martin, D. S. Prono, and A. G. Cole, Phys. Rev. Lett **57**, 13 (1986).

[4]R. F Lucey, Jr., R. M. Gilgenbach, J. D. Miller, J. E. Tucker, and R. A. Bosch, Phys. Fluids B **1**, 430 (1989).

[5]D. H. Whittum, A. M. Sessler and J. M. Dawson, Phys. Rev. Lett. **64**, 2511 (1990).

[6]K. R. Chen, T. Katsouleas, and J. M. Dawson, IEEE Trans. Plasma Sci. **18**, 837 (1990).

[7]D. H. Whittum, Ph. D. thesis, University of California at Berkeley, 1990.

[8]C. A. Frost, J. R. Woodworth, J. N. Olsen And T. A. Green, Appl. Phys. Lett. **41**, 813 (1982).

[9]N. M. Kroll, P. L. Morton, and M. N. Rosenbluth, IEEE J. Quant. Elec. **QE-17**, 1436 (1981).

[10]K. R. Chu and J. L. Hirshfield, Phys. Fluids **21**, 461 (1978).

[11]R. Bonifacio, C. Pellegrini, and L. M. Narducci, Opt. Commun. **50**, 373 (1984).

[12]T.J. Orzechowski, E. T. Scharlemann, B. Anderson, V. K. Neil, W. M. Fawley, D. Prosnitz, S. M. Yarema, D. B. Hopkins, A. C. Paul, A. M. Sessler, and J. S. Wurtele, IEEE J. Quant. Elec. **QE-21**, 831 (1985).

[13]This result and the solution for the eikonal in this limit are identical to that for the cold-beam FEL. W. B. Colson and A. M. Sessler, Ann. Rev. Nucl. Part. Sci. **35**, 25 (1985).

[14]This has an analog in the FEL, where the instability is stabilized for finite positive detuning. N. M. Kroll and W. A. McMullin, Phys. Rev. A **17**, 300 (1978). See in particular, Eqs. (3.19) and (3.20), and related discussion.

[15]S. Hiramatsu, K. Ebihara, Y. Kimura, J. Kishiro, M. Kumada, H. Kurino, Y. Mizumachi, T. Ozaki and K. Takayama, Nucl. Instrum. Methods **A285**, 83 (1989).

[16]B. W. Montague and W. Schnell, in *Laser Acceleration of Particles*, edited by Chan Joshi and Thomas Katsouleas, AIP Conf. Proc. **130**, (AIP, New York, 1985), p. 146.

[17]T. P. Hughes and B. B. Godfrey, Phys. Fluids **27**, 1531 (1984).

[18]W. M. Sharp and M. Lampe, Phys. Fluids **23**, 2383 (1980).

[19] A. M. Sessler, D. H. Whittum and L.-H. Yu, "Radio-Frequency Beam Conditioner for Fast-Wave Free-Electron Generators of Coherent Radiation" (submitted to Phys. Rev. Lett.).

[20]B. Levush, T.M. Antonsen, W.M. Manheimer, and P. Sprangle, Phys. Fluids **28**, 2273 (1985); T.P. Hughes and B.B. Godfrey, Phys. Fluids **29**, 1698 (1985); T. Antonsen and B. Levush, IEEE J. Quant. Electron. **QE-23**, 1621 (1987).

[21]P. E. Latham, Phys. Fluids B **1**, 2085 (1989).

[22]C. M. Tang, P. Sprangle, J. Krall, P. Serafim and F. Mako, Particle Acclerators **35**, 101 (1991); J. Krall, C. M. Tang, G. Joyce and P. Sprangle Phys. Fluids B **3**, 204 (1991); C. M. Tang and J. Krall, "Electromagnetic Instability of an Intense Beam in a Quadrupole Focussing System-Theory and Simulation", to be published in *Proceedings of the 1991 IEEE Particle Accelerator Conference*, (IEEE, New York, 1991).

[23]K. G. Kato, G. Benford, D. Tzach, Phys. Rev. Lett. **50**, 1587 (1983).

[24]M. S. Di Capua, J. F. Camacho, E. S. Fulkerson, and D. Meeker, IEEE Trans. Plasma Sci. **16**, 217 (1988).

[25]A. N. Lebedev and G. V. Martirosyan, Sov. Phys. Tech. Phys. **26**, 1085 (1981); G. V. Martirosyan, Sov. J. Tech. Phys. **53**, 699 (1983).

[26]D. H. Whittum, Simon S. Yu, William M. Sharp, M. Lampe, "Electron-hose instability in the ion-focussed regime", Lawrence Berkeley Laboratory Report No. 29521 (submitted to Phys. Rev. Lett.).

[27]E. T. Scharlemann, A. M. Sessler, and J. M. Wurtele, Phys. Rev. Lett. **54**, 1925 (1985).

[28]G. T. Moore, Opt. Comm. **52**, 46 (1984), and **54**, 121 (1985).

[29]M. Xie and D. A. G. Deacon, Nucl. Instrum. Methods **A250**, 426 (1986).

**Table I.** Parameters for an ion-channel microwave amplifier.

| | | |
|---|---|---|
| beam energy | $E$ | 1 MeV |
| beam current | $I$ | 4 kA |
| rms emittance | $\varepsilon_n$ | 0.25 cm-rad |
| beam radius | $a$ | 1.4 cm |
| betatron period | $\lambda_\beta$ | 30 cm |
| betatron parameter | $a_\beta$ | 0.5 |
| plasma density | $n_p$ | $6 \times 10^{10}$ cm$^{-3}$ |
| signal wavelength | $\lambda$ | 3.2 cm |
| input power | $P_i$ | 50 kW |
| waveguide width | $w_x$ | 11 cm |
| waveguide height | $w_y$ | 5.5 cm |

**FIG. 1.** A relativistic electron beam propagates through a preionized plasma, less dense than the beam core. (a) All plasma electrons are expelled from the beam volume, by the beam head (flared portion) leaving a non-neutral column of ions or "ion-channel" to focus the remainder of the beam. (b) A cross-section of the beam well-removed from the beam head. The beam radius is $a$, and the ion-channel extends out to the laser waist $b>a$.

**FIG. 2.** An electromagnetic wave propagates with an ion-focused relativistic electron beam. Beam electrons oscillate transversely and are perturbed axially by the ponderomotive force, much as in an FEL. Unlike the FEL, the perturbation to the transverse motion (via the relativistic mass effect and the transverse Lorentz force) is important to an understanding of instability growth.

**FIG. 3.** The solution of the dispersion relation, Eq. (60), for the normalized growth rate $\zeta_i = Im(\zeta_+) = Re(\Gamma_+)/k_\beta$, plotted versus detuning, $\delta$ and the parameter $\mu$, for $-100<\delta/\rho<50$ and $0<\mu/\rho<20$. The peak value $\zeta_i = 3^{1/2}$ occurs at $\delta=\mu=0$.

**FIG. 4.** Solution of Eq. (60) for (a) the maximum growth rate $Im(\zeta_+)$ and (b) the corresponding detuning, $\delta$, plotted versus $\mu$. All quantities are normalized by the Pierce parameter $\rho$.

**FIG. 5.** Results of the simulations ECL (smooth curve) and FCL for microwave power $P$, versus axial displacement along the beam line, $z$ for the example of Table I. The oscillatory character of the FCL result is due to the jitter motion discussed in connection with Eq. (17).

**FIG. 6.** (a) Result of the simulation FCL for $y$-momentum averaged over the ensemble. Near saturation, the beam develops a coherent oscillation consistent with Eq. (65). (b) FCL result for the rms normalized emittance in $y$. Emittance in $y$ is reduced near saturation, as discussed in connection with Eq. (39).

**FIG. 7.** Results of the simulation ECL for power at saturation and length for saturation versus detuning spread $\delta_s$, at zero center detuning. These results confirm that a detuning spread $\delta_s < \rho$ has only a small effect on the output power.

**FIG. 8.** Results of the simulation ECL for power at saturation and length for saturation versus center detuning $\delta_0$, for a fixed detuning spread $\delta_s = 15\% \sim 2\rho$. Higher gain occurs for $\delta_0 < 0$, consistent with Fig. 4.

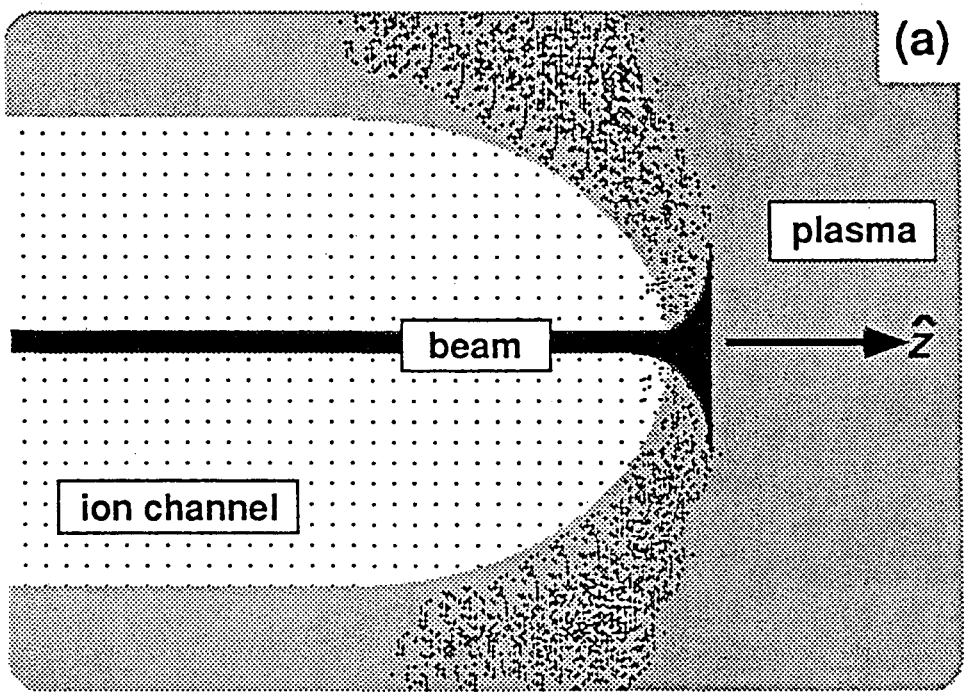


FIG. 1(a)

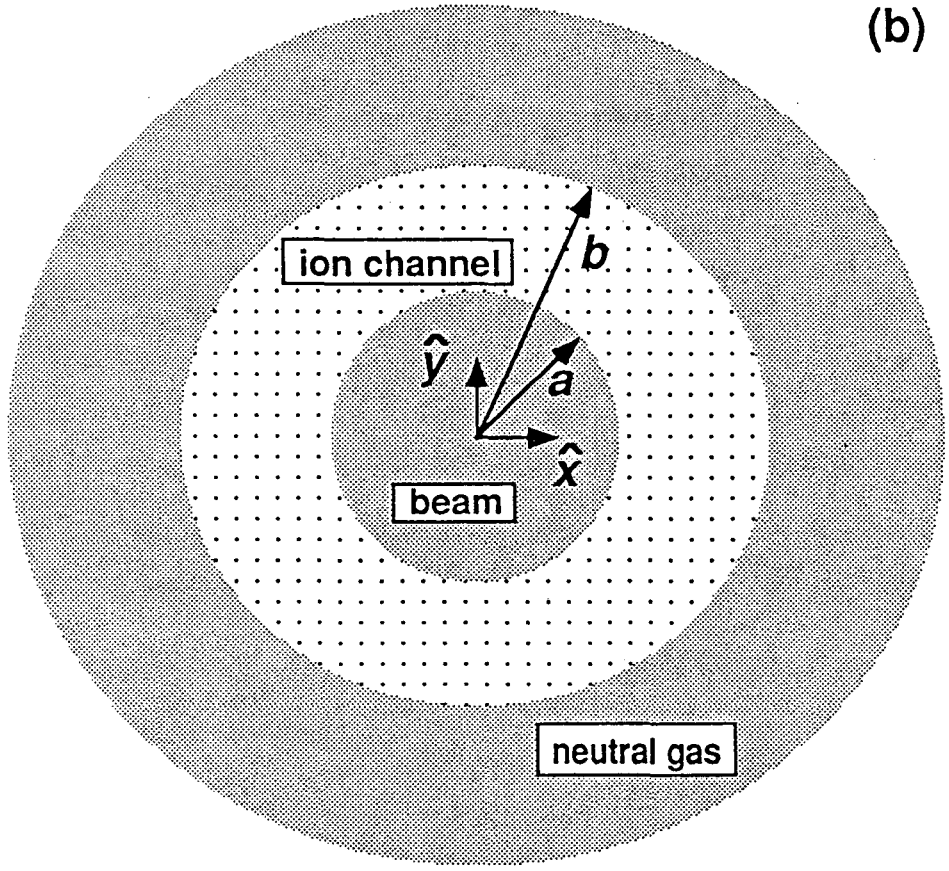


FIG. 1(b)

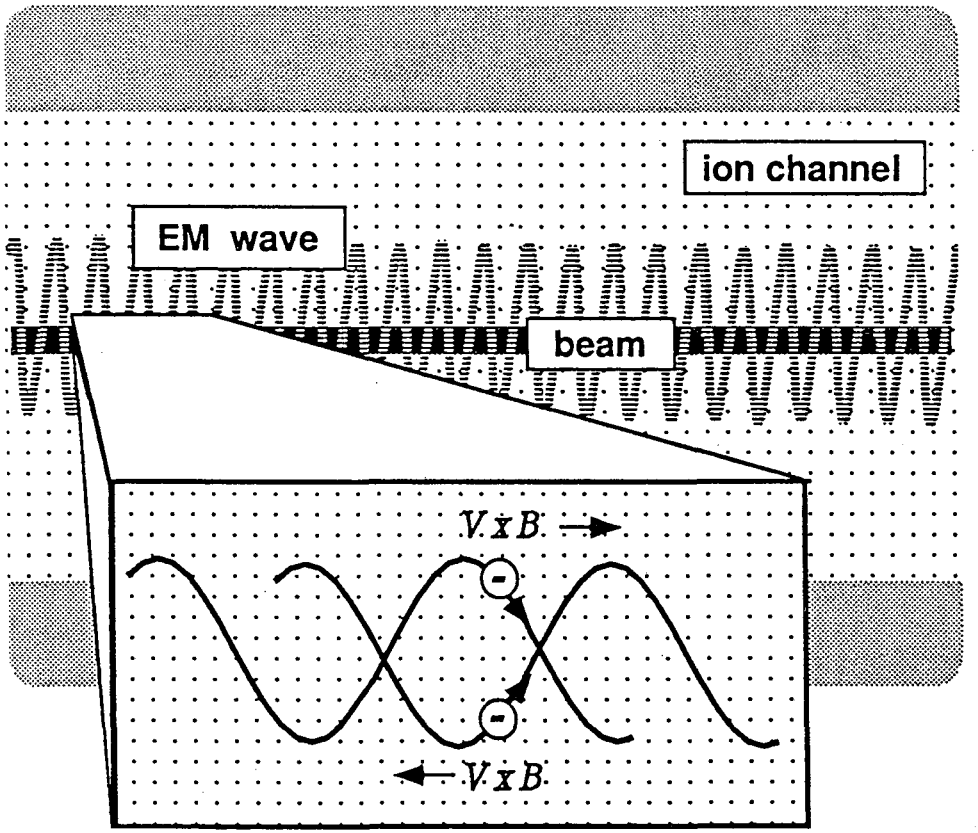


FIG. 2

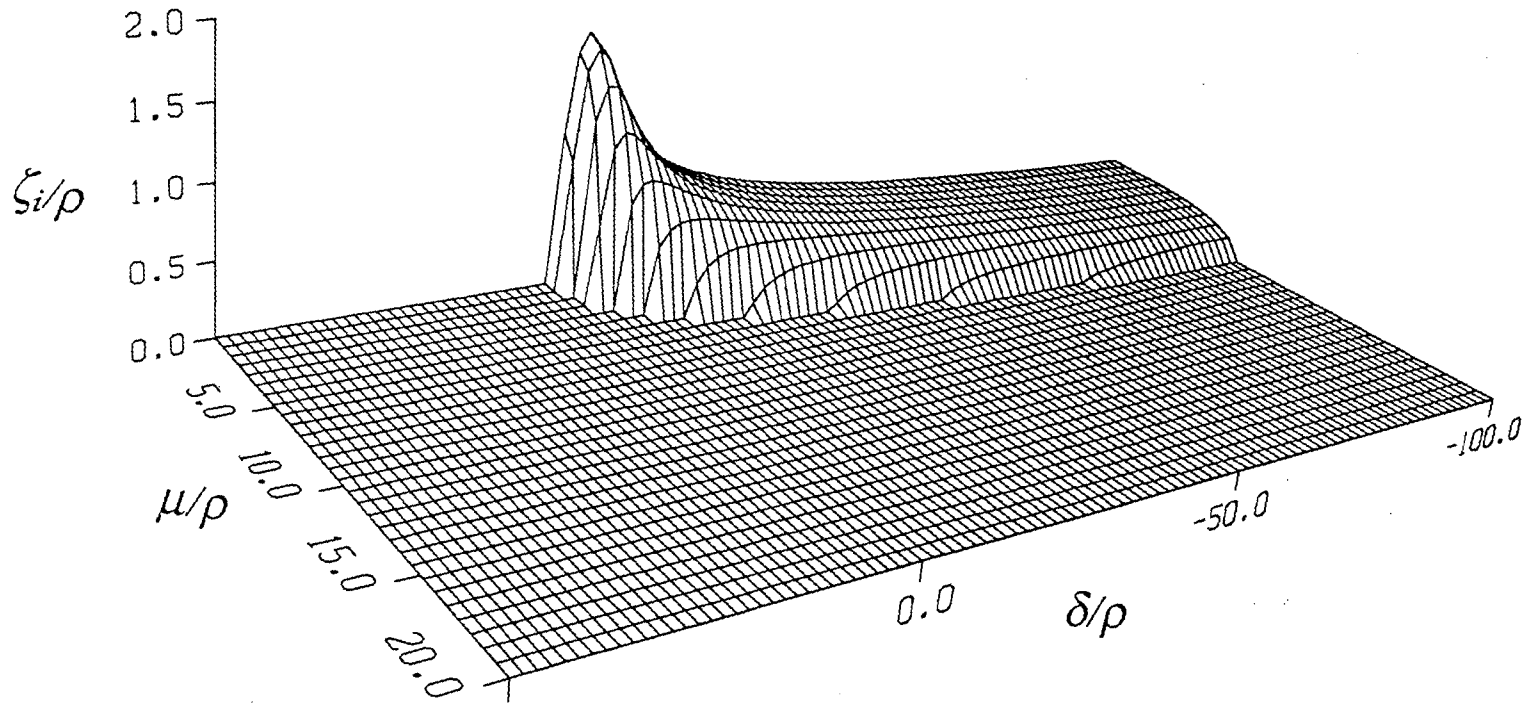
2.0
1.5
1.0
0.5
0.0
$\zeta_i/\rho$
5.0
10.0
15.0
20.0
$\mu/\rho$
0.0
-50.0
-100.0
$\delta/\rho$

FIG. 3

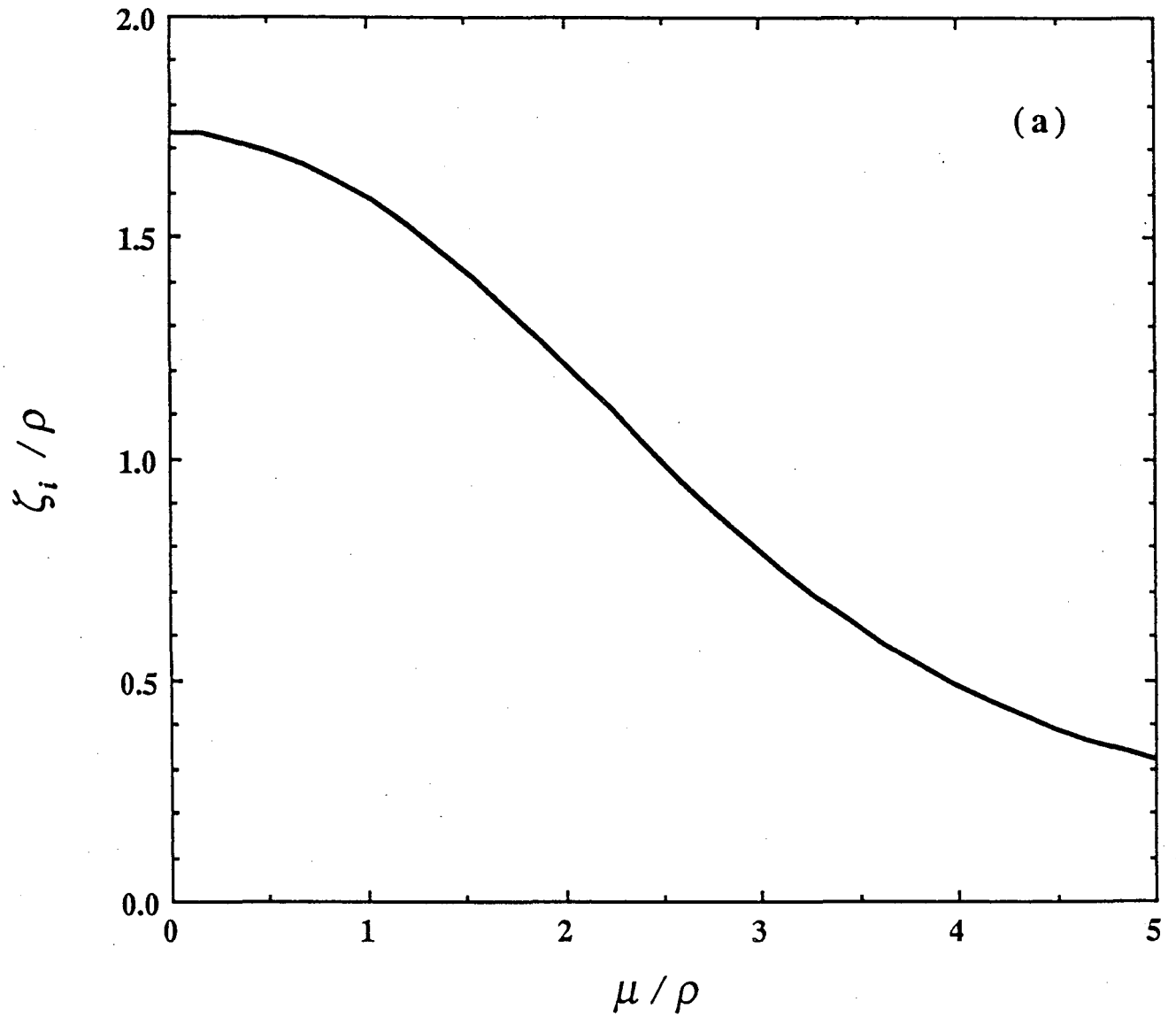


FIG. 4(a)

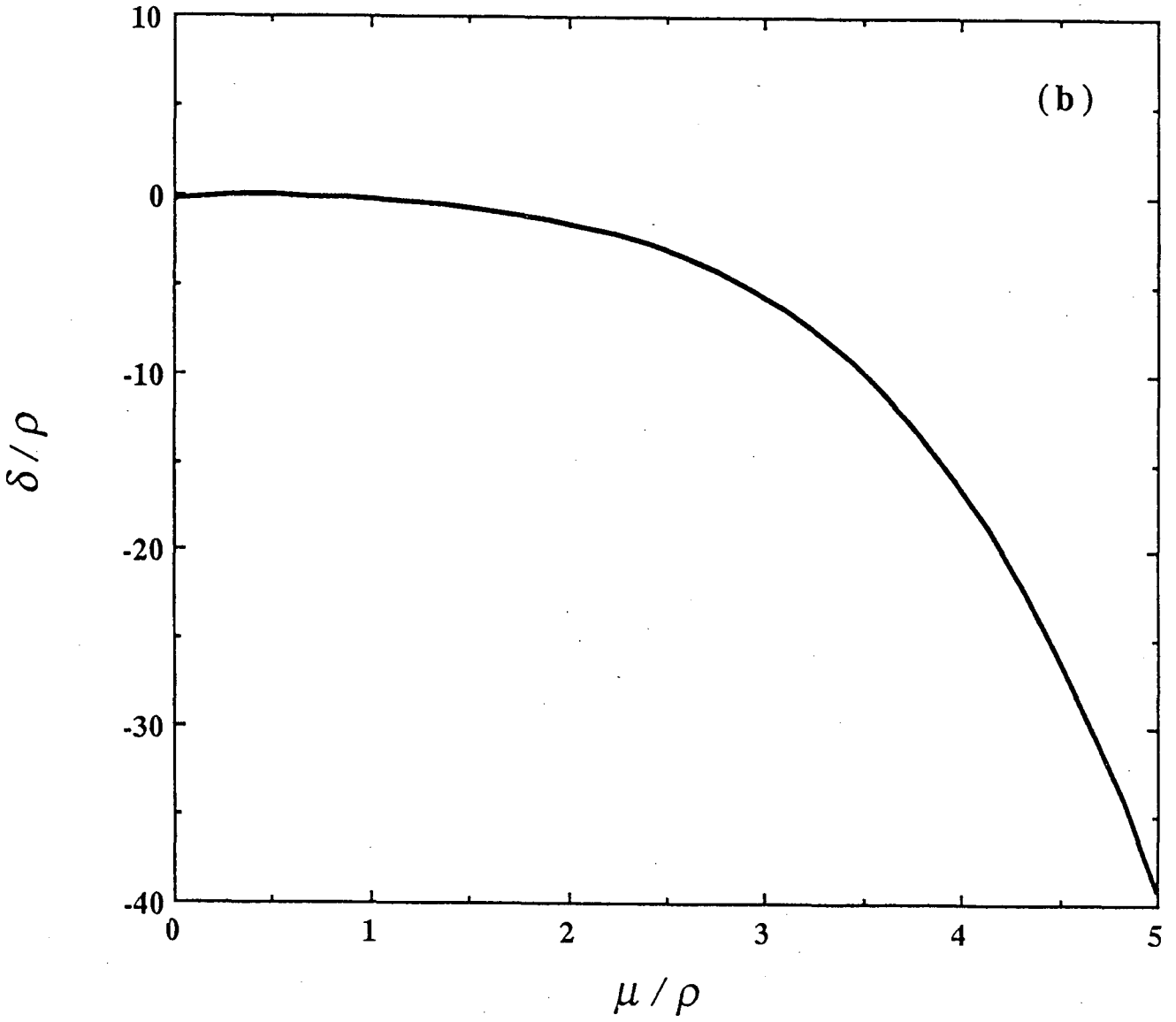


FIG. 4(b)

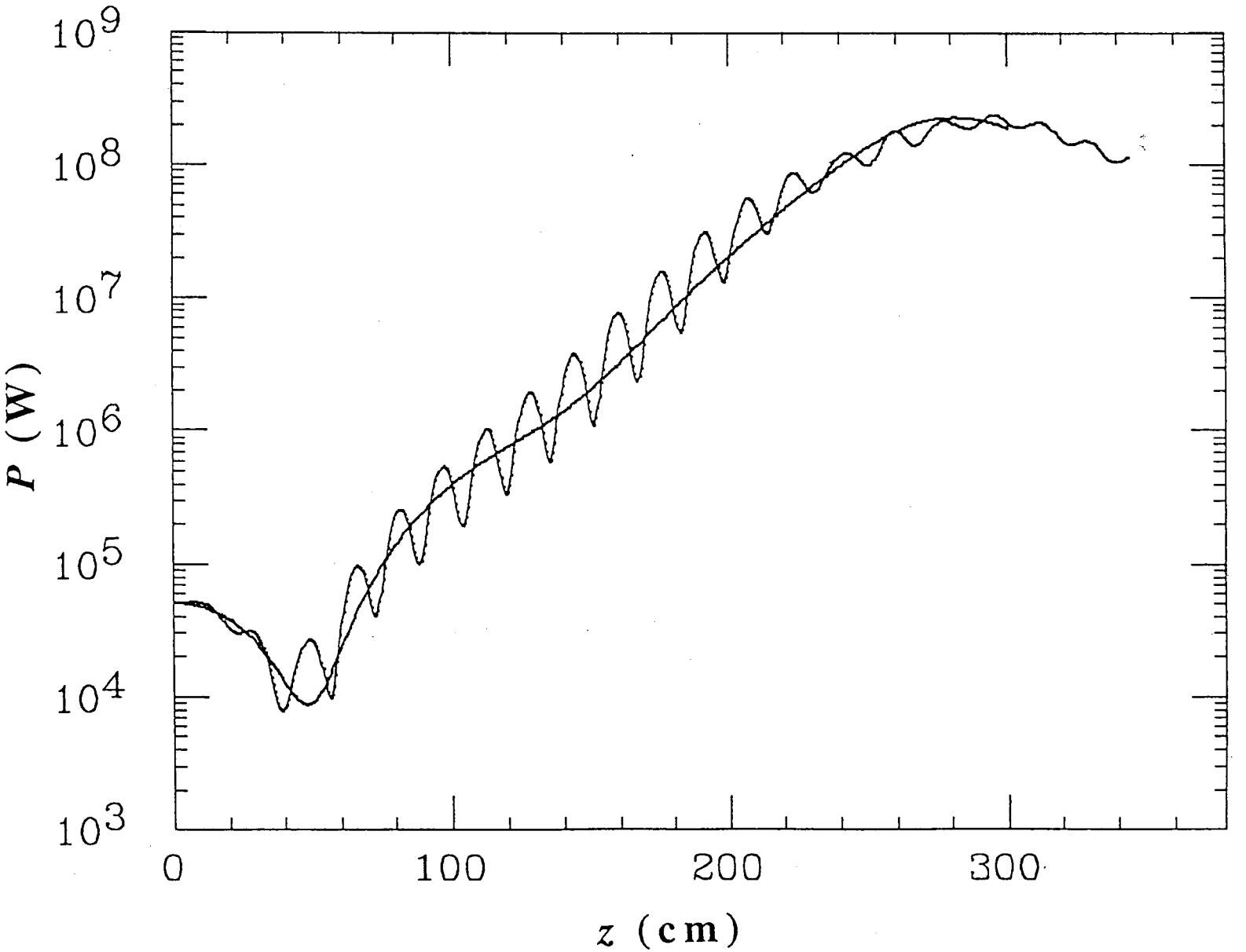


FIG. 5

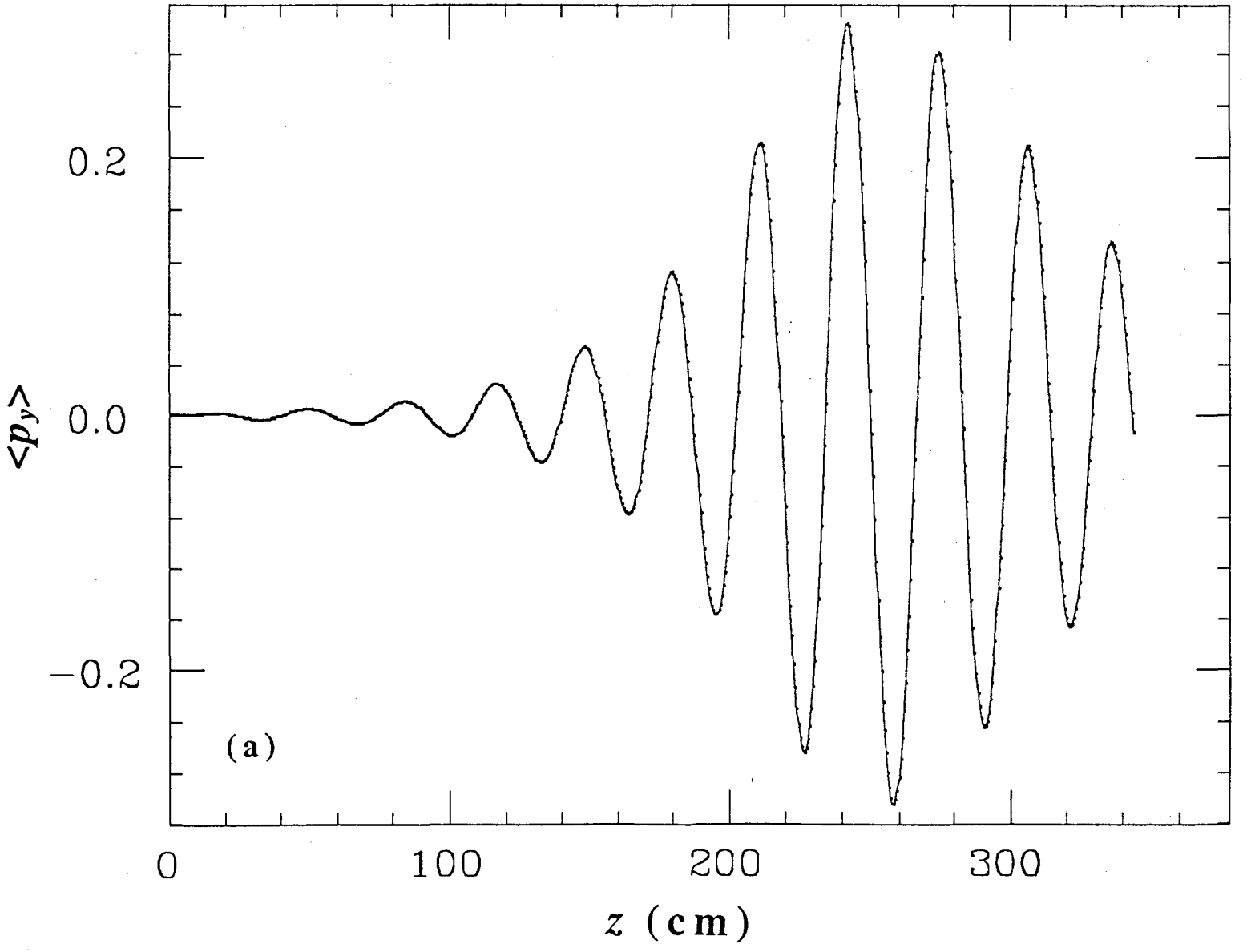


FIG. 6(a)

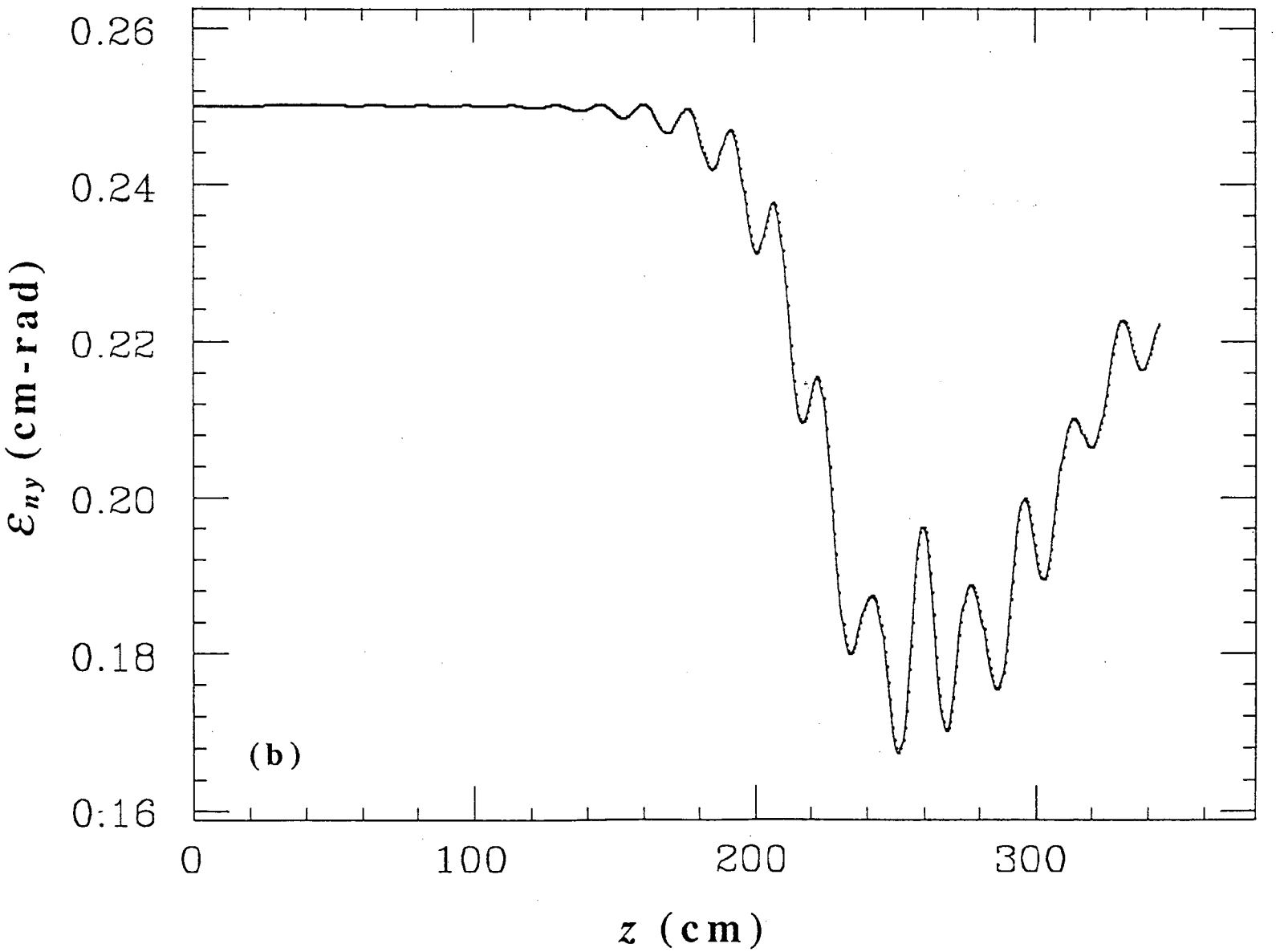


FIG. 6(b)

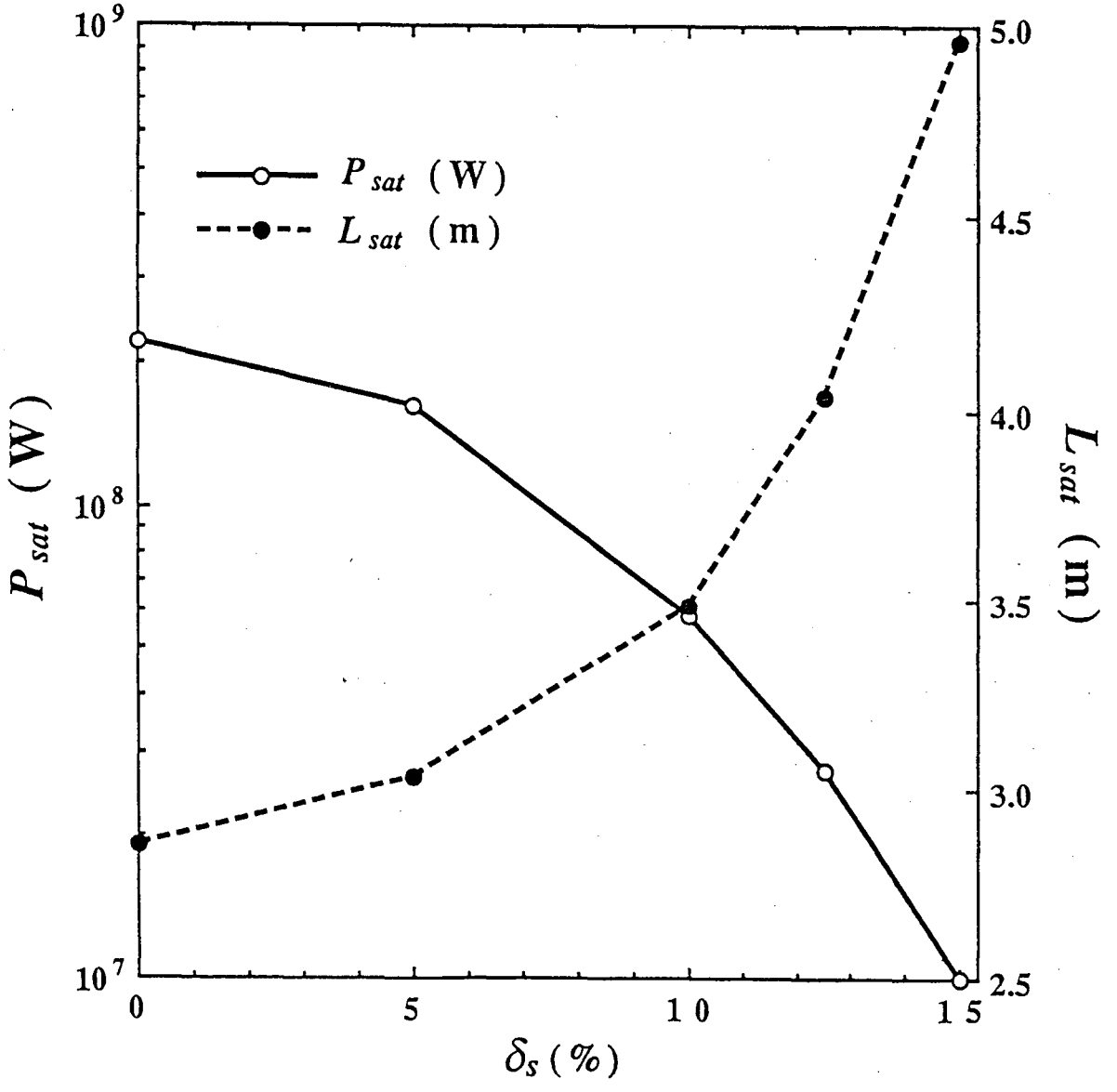
$10^9$
$10^8$
$10^7$
$P_{sat}$ (W)
5.0
4.5
4.0
3.5
3.0
2.5
$L_{sat}$ (m)
0
5
10
15
$\delta_s$ (%)
$P_{sat}$ (W)
$L_{sat}$ (m)

FIG. 7

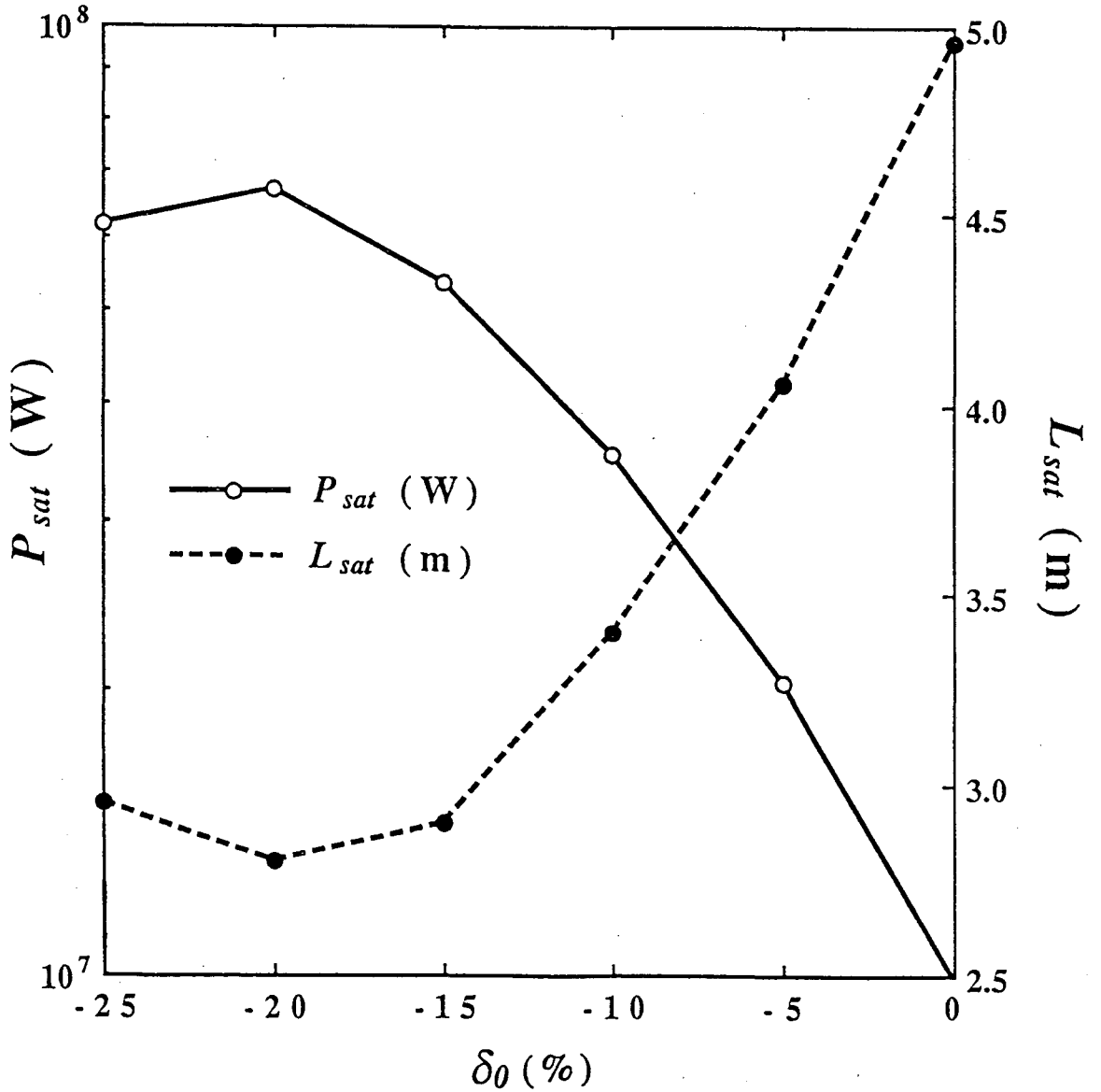
$10^8$
$10^7$
$P_{sat}$ (W)
$L_{sat}$ (m)
5.0
4.5
4.0
3.5
3.0
2.5
-25
-20
-15
-10
-5
0
$\delta_0$ (%)
$P_{sat}$ (W)
$L_{sat}$ (m)

FIG. 8

LAWRENCE BERKELEY LABORATORY
UNIVERSITY OF CALIFORNIA
INFORMATION RESOURCES DEPARTMENT
BERKELEY, CALIFORNIA 94720